Journal of Molecular Catalysis A: Chemical 326 (2010) 48–54

Contents lists available at ScienceDirect

Journal of Molecular Catalysis A: Chemical

journal homepage: www.elsevier.com/locate/molcata

Gas phase hydrogenation of nitroarenes: A comparison of the catalytic action of titania supported gold and silver

Fernando Cárdenas-Lizana[a], Zahara M. de Pedro[b], Santiago Gómez-Quero[a], Mark A. Keane[a,*]

[a] Chemical Engineering, School of Engineering and Physical Sciences, Heriot-Watt University, Edinburgh EH14 4AS, Scotland, United Kingdom
[b] Ingeniería Química, Facultad de Ciencias, Universidad Autónoma de Madrid, Cantoblanco, 28049 Madrid, Spain

ARTICLE INFO

Article history:
Received 12 January 2010
Received in revised form 15 March 2010
Accepted 11 April 2010
Available online 18 April 2010

Keywords:
Au/TiO_2
Ag/TiO_2
Selective hydrogenation
Nitroarenes
Hammett equation

ABSTRACT

We have examined the catalytic action of 1 mol% Au/TiO_2 and Ag/TiO_2 in the continuous gas phase hydrogenation of a series of *para*-substituted (–H, –OH, $–OCH_3$, $–CH_3$, –Cl and $–NO_2$) nitroarenes. Both catalysts promoted exclusive $–NO_2$ group reduction, resulting in the sole formation of the corresponding amino-compound. The catalysts have been characterized in terms of temperature-programmed reduction (TPR), H_2 chemisorption, BET area, diffuse reflectance UV–vis, X-ray diffraction and HRTEM measurements. The formation of zero valent Au and Ag is established post-TPR. Au/TiO_2 showed a narrower metal particle size (1–10 nm) distribution than Ag/TiO_2 (1–15 nm) but both catalysts exhibited a similar surface area weighted mean size (6–7 nm). A time-invariant nitroarene conversion has been established where Au/TiO_2 delivered higher specific hydrogenation rates. We associate this response to an enhanced reactant activation on Au/TiO_2 to generate a negatively charged intermediate, consistent with a nucleophilic mechanism. The presence of electron-withdrawing substituents is shown to enhance $–NO_2$ reduction rate. This effect is quantified in terms of the Hammett relationship where a linear correlation between the substituent constant (σ_i) and rate is established and a higher reaction constant (ρ) was recorded for Au/TiO_2 (0.93) relative to Ag/TiO_2 (0.22). The data generated provide the first direct comparison of the catalytic action of supported Au and Ag in the hydrogenation of substituted nitroarenes and establish the viability of both catalysts to promote selective $–NO_2$ group reduction.

1. Introduction

The catalytic hydrogenation of poly-functional nitro-compounds to the corresponding amino-product is of commercial importance in the manufacture of a diversity of herbicides, dyes and pharmaceuticals [1]. Exclusivity in terms of $–NO_2$ group reduction is difficult to achieve in the presence of other reactive substituents (*e.g.* –Cl, $–CH_3$ and/or –OH), as has been noted for the hydrogenation of a range of aliphatic [2] and aromatic [3] nitro-compounds in both gas [4,5] and liquid [6,7] phase operation. The conventional synthesis route for amino-derivates, using stoichiometric amounts of Fe in acid media (Béchamp process) is no longer sustainable due to the production of Fe/FeO sludge waste and low selectivites/product yields [8]. The catalytic (liquid phase) alternative using standard transition metals (*e.g.* Ni [9], Pd [10], and/or Pt [7]) also exhibits limitations in terms of undesirable toxic secondary reaction products, *i.e.* azo- [11] and/or azoxy-derivates [12]. Various attempts have been reported to enhance selectivity to the target amino-compound, through the use of additives [13], variations in catalyst preparation [9,14] and the incorporation of a second metal [15,16]. Gold and (to a lesser extent) silver have been successfully used in the hydrogenation of CO_2 [17], NO_x [18,19], alkenes [20] and α,β-unsaturated aldehydes [21,22]. Moreover, recent studies of batch liquid phase nitroarene reduction over supported Au [14,23] and Ag [24–26] show potential in terms of high selectivity to amino-compound formation. We have previously demonstrated exclusive -NO_2 group reduction in the hydrogenation of chloro- [4,27–29] and dinitro-benzene [30] over supported Au in continuous gas phase operation. To the best of our knowledge, the catalytic action of supported Ag in the gas phase hydrogenation of nitro-compounds has not been reported in the literature. In this study, we compare the catalytic performance of (titania) supported Ag and Au in the hydrogenation of a series of substituted nitro-compounds to commercially important amino-derivates.

In general, supported Au [17,31,32] and/or Ag [17,21,33] exhibit lower hydrogenation activities relative to typical transition metal catalysts, *e.g.* supported Ni [31], Pd [33], Pt [32] or Rh [21]. There is evidence [22,34–36] of a structure sensitive response in the case of Au where increased efficiency is attributed to smaller particles (≤10 nm). Theoretical calculations have demonstrated a high energy barrier for H_2 dissociation on group IB metals [37] and, in

* Corresponding author. Tel.: +44 0131 4514719.
E-mail address: M.A.Keane@hw.ac.uk (M.A. Keane).

1381-1169/$ – see front matter © 2010 Elsevier B.V. All rights reserved.
doi:10.1016/j.molcata.2010.04.006

the case of Au catalysts, H_2 activation has been associated with step, edge and corner sites on small Au particles [38]. While we could not find any study that explicitly compares the catalytic performance of Au with Ag in nitroarene reduction, we can flag related reports dealing with hydrogen-mediated reactions. Deng et al. [39] studied the hydrogenation of anthracene with $NaBH_4$ as reducing agent over (unsupported) Ag and Au nano-particles and achieved higher rates over the former for particles below 4 nm, a response that they associated with a greater capacity of Ag to generate hydrogen for reaction. Słoczyński et al. [17] considered M/($ZnO{\cdot}ZrO_2$) (M = Cu, Au and Ag; mole ratio ZnO/ZrO_2 = 3) and reported a similar yield of methanol (from CO_2) over the Au and Ag catalysts that was lower than that for Cu/($ZnO{\cdot}ZrO_2$), attributing this response to a low stabilization of the Ag^+ and Au^+ ions under reaction conditions. In contrast, Wambach et al. [40] observed the exclusive formation of methanol over Ag/ZrO_2 while methane, methanol and CO were generated over Au/ZrO_2. We provide, in this report, a direct comparison of titania supported Au and Ag (at 1 mol% loading) in the selective hydrogenation of a series of *para*-substituted nitroarenes where the catalytic response has been correlated to critical characterization measurements.

2. Experimental

2.1. Materials and catalyst preparation

The TiO_2 (Degussa, P25) support was used as received. Two (1 mol%) TiO_2 supported Au and Ag catalyst precursors were prepared by standard impregnation where adequate volumes of $HAuCl_4$ (Aldrich, 25×10^{-3} g cm^{-3}, pH = 2) and $AgNO_3$ (Riedel-de Haën, 1×10^{-3} g cm^{-3}) solutions were added to 5 g of support. The slurry was heated (2 K min^{-1}) to 353 K and maintained under constant agitation (600 rpm) in a He purge. The solid residue was dried in a flow of He at 383 K for 3 h and stored under He in the dark at 277 K. Prior to use in catalysis, the samples (sieved into a batch of 75 μm average diameter) were activated in 60 cm^3 min^{-1} H_2 at 2 K min^{-1} to 603 ± 1 K, which was maintained for 2.5 h. After activation, the samples were cooled and passivated in 1% (v/v) O_2/He at 298 K for off-line analysis.

2.2. Characterization analyses

Temperature-programmed reduction (TPR) response, BET area and H_2 chemisorption measurements were recorded using the commercial CHEMBET 3000 (Quantachrome Instrument) unit with data acquisition/manipulation using the TPR Win™ software. The samples were loaded into a U-shaped Pyrex glass cell (100 mm × 3.76 mm i.d.) and heated in 17 cm^3 min^{-1} (Brooks mass flow controlled) 5% (v/v) H_2/N_2 to 603 K at 2 K min^{-1}. The effluent gas passed through a liquid N_2 trap and changes in H_2 consumption were monitored by TCD (thermal conductivity detector). The reduced samples were swept with 65 cm^3 min^{-1} N_2 for 1.5 h, cooled to room temperature and subjected to H_2 chemisorption using a pulse (10–50 μl) titration procedure. Hydrogen pulse introduction was repeated until the signal area was constant, indicating surface saturation. BET areas were recorded with a 30% (v/v) N_2/He flow; pure N_2 (99.9%) served as the internal standard. At least two cycles of N_2 adsorption–desorption in the flow mode were used to determine total surface area using the standard single point method. BET surface area and H_2 uptake values were reproducible to within ±5% and the values quoted in this paper represent the mean. Powder X-ray diffractograms were recorded on a Bruker/Siemens D500 incident X-ray diffractometer using Cu Kα radiation. The samples were scanned at a rate of 0.02° step^{-1} over the range $20° \leq 2\theta \leq 90°$ (scan time = 5 s step^{-1}). Diffractograms were identified using the JCPDS-ICDD reference standards, *i.e.* anatase (21-1272), rutile (21-1276), Au (04-0784) and Ag (04-0783). Diffuse reflectance UV–vis (DRS UV–vis) measurements were conducted using a PerkinElmer Lambda 35 UV-vis Spectrometer with $BaSO_4$ powder as reference; absorption profiles were calculated from the reflectance data using the Kubelka–Munk function. Transmission electron microscopy analysis was conducted using a JEOL JEM 2011 HRTEM unit with a UTW energy dispersive X-ray detector (EDX) (Oxford Instruments) operated at an accelerating voltage of 200 kV, employing Gatan DigitalMicrograph 3.4 for data acquisition/manipulation. Samples for analysis were prepared by dispersion in acetone and deposited on a holey carbon/Cu grid (300 mesh). Up to 600 individual metal particles were counted for each catalyst and the surface area-weighted metal diameter (d_{TEM}) was calculated from

$$d_{TEM} = \frac{\sum_i n_i d_i^3}{\sum_i n_i d_i^2} \quad (1)$$

where n_i is the number of particles of diameter d_i. The size limit for the detection of metal particles on TiO_2 is *ca.* 1 nm.

2.3. Catalytic procedure

Reactions were carried out under atmospheric pressure, *in situ* immediately after activation, in a fixed bed vertical continuous glass reactor (l = 600 mm, i.d. = 15 mm) at T = 473 K. The catalytic reactor, and operating conditions to ensure negligible heat/mass transport limitations, have been fully described elsewhere [41] but some features, pertinent to this study, are given below. A preheating zone (layer of borosilicate glass balls) ensured that the nitroarene reactant was vaporized and reached reaction temperature before contacting the catalyst. Isothermal conditions (±1 K) were maintained by thoroughly mixing the catalyst with ground glass (75 μm) before insertion into the reactor. The temperature was continuously monitored by a thermocouple inserted in a thermowell within the catalyst bed. Butanolic solutions of the nitroarene reactants were delivered, in a co-current flow of H_2, *via* a glass/teflon air-tight syringe and a teflon line, using a microprocessor controlled infusion pump (Model 100 kd Scientific) at a fixed calibrated flow rate, with an inlet $-NO_2$ molar flow (F_{-NO_2}) over the range 0.01–0.11 mmol$_{-NO_2}$ h^{-1}, where the molar metal to inlet molar $-NO_2$ feed rate ratio spanned the range 2×10^{-2}–27×10^{-2} h. The H_2 content was at least 150 times in excess of the stoichiometric requirement, the flow rate of which was monitored using a Humonics (Model 520) digital flowmeter; GHSV = 2×10^4 h^{-1}. In a series of blank tests, passage of each nitroarene in a stream of H_2 through the empty reactor or over the support alone, *i.e.* in the absence of Au or Ag, did not result in any detectable conversion. The reactor effluent was frozen in a liquid nitrogen trap for subsequent analysis, which was made using a PerkinElmer Auto System XL gas chromatograph equipped with a programmed split/splitless injector and a flame ionization detector, employing a DB-1 50 m × 0.20 mm i.d., 0.33 μm film thickness capillary column (J&W Scientific), as described elsewhere [42]. The reactants: nitrobenzene, *p*-nitrophenol, *p*-nitroanisole, *p*-nitrotoluene, *p*-chloronitrobenzene and *p*-dinitrobenzene (Aldrich, ≥98%) and the solvent (1-butanol: Riedel-de Haën) were used as supplied without further purification. Repeated catalytic runs with different samples from the same batch of catalyst delivered product compositions that were reproducible to within ±6%. Hydrogenation activity is expressed in terms of the degree of nitro-group reduction

Table 1
BET surface area, hydrogen consumed (theoretical and experimentally determined) during activation by TPR, H_2 chemisorption values, DRS UV–vis characteristics, metal particle size (surface area weighted mean and range), specific metal surface area and pseudo-first order rate constants for the hydrogenation of nitrobenzene (to aniline) associated with Au/TiO_2 and Ag/TiO_2.

Catalyst	Au/TiO_2	Ag/TiO_2
BET area ($m^2\,g^{-1}$)	47	48
TPR H_2 consumption/theoretical ($\mu mol\,g^{-1}$)	193	130
TPR H_2 consumption/experimental ($\mu mol\,g^{-1}$)	195	136
H_2 chemisorption ($\mu mol\ g^{-1}_{metal}$)	15	5
DRS UV–vis A_{max} (nm)	568	450
d_{TEM} (nm)	6.1	7.3
S_{metal} ($m^2_{metal}\,g^{-1}_{metal}$)[a]	53	82
Metal size range (nm)	1–10	1–15
$k_{473\,K}$[b] ($k'_{473\,K}$)[c]	2[b] (15×10^{-5})[c]	1[b] (12×10^{-5})[c]

[a] $S_{metal} = 6/(\rho_{metal} \times d_{TEM})$ where $\rho_{Au} = 18.88\,g\,cm^{-3}$; $\rho_{Ag} = 10.50\,g\,cm^{-3}$.
[b] Units $= mol_{-NO_2}\,mol^{-1}_{metal}\,h^{-1}$.
[c] Units $= mol_{-NO_2}\,m^{-2}_{metal}\,h^{-1}$.

(x_{-NO_2})

$$x_{-NO_2} = \frac{[-NH_2]_{out}}{[-NO_2]_{in}} \quad (2)$$

where the subscripts *in* and *out* refer to the inlet and outlet streams.

3. Results and discussion

3.1. Catalyst characterization

The results of the BET surface area, room temperature H_2 chemisorption, DRS UV–vis measurements along with the mean metal particle sizes (and range of values) obtained from TEM analysis are given in Table 1. In terms of TPR analysis, the experimentally determined hydrogen consumption is also provided and can be compared with the predicted (or theoretical) values based on the precursor loading. The TPR profiles generated for Au/TiO_2 (AI) and Ag/TiO_2 (BI) are shown in Fig. 1. In the case of Au/TiO_2, hydrogen consumption matched (within 1%) that required for the reduction of $HAuCl_4$ to the metallic form. This result agrees with reports in the literature where the reduction of Au^{3+} to Au^0 at $T \leq 503$ K has been proposed [27,43–45] for oxide (Al_2O_3 and/or TiO_2) supported Au prepared by impregnation. Hydrogen consumption during TPR in the case of Ag/TiO_2 is consistent with a two-step reduction mechanism, *i.e.* $AgNO_3 \rightarrow Ag_2O \rightarrow Ag^0$, as has been suggested for Ag supported on TiO_2 [46], Al_2O_3 [47], SiO_2 [48] and carbon [49]. Bogdanchikova et al. [50] examined an Ag/Al_2O_3 precursor prepared by impregnation with $AgNO_3$ and established (by XRD) that Ag^0 was not present in the precursor, demonstrating metallic Ag formation post-TPR to 673 K. The room temperature H_2 chemisorption values recorded for both catalysts were close to the instrument detection limits but the uptake on Ag/TiO_2 was measurably lower. These values are in keeping with the low capacity of Au [4,37] and Ag [51,52] for H_2 uptake due to the filled *d*-band [35,53]. The DRS UV–vis spectra for the passivated/reduced samples are shown in Fig. 1. The spectrum for Au/TiO_2 (AII) exhibits an absorption band at 568 nm that is characteristic of Au nanoclusters on a titania substrate [54]. The spectrum for Ag/TiO_2 (BII) presents an absorption band at 450 nm, which can be linked to the presence of Ag^0. Indeed, wavelengths >390 nm have been attributed elsewhere [24,50] to the presence of metallic Ag particles. Jia et al. [55] have associated a band at 420 nm to absorbance by Ag nano-particles, where a displacement to higher wavelengths was ascribed to an increase in particle size (from 6 nm to 18 nm). The XRD profiles for passivated/reduced Au/TiO_2 (AIII) and Ag/TiO_2 (BIII) are also presented in Fig. 1. Both systems exhibit signals at $2\theta = 25.3°$, 37.8° and 48.1° corresponding to the (1 0 1), (0 0 4) and (2 0 0) planes of tetragonal anatase (JCPDS-ICDD 21-1272). Moreover, the peak at 27.4° is diagnostic of a tetragonal rutile content (JCPDS-ICDD 21-1276). This XRD response is consistent with a mixture of anatase (80% volume fraction) and rutile forms of TiO_2 in agreement with the reported [56] Degussa, P25 composition. It is important to note that only weak signals (overlapping with the (0 0 4) anatase peak) due to metallic Au and Ag ($2\theta = 38.1°$) were distinguishable, a result that suggests a highly dispersed metallic phase.

In the case of titania supported metals, a migration of Ti suboxide species to occlude the metal particles can occur at elevated temperature (≥773 K) and has been described in terms of an encapsulation or decoration [57]. We observed a similar effect in our TEM analysis after prolonged electron beam irradiation. This is illustrated for Au/TiO_2 in Fig. 2. In both images, an encapsulation of Au nano-particles is in evidence. Indeed, in image (II) atomic layers of the support can be seen (indicated by arrows) surrounding an isolated Au particle. The diffractogram patterns for a selected area of the support and an Au particle are shown in images (IA) and (IB), respectively. In both cases, the *d*-spacing obtained (*ca.* 0.35 nm) are close to that associated with the characteristic (1 0 1) main plane of TiO_2-anatase (JCPDS-ICDD 21-1272). Metal encapsulation as a result of analytical TEM measurements has been previously demonstrated for Au/CeO_2 [58] but we provide here, for the first time, evidence of such an effect in the case of Au/TiO_2. In order to circumvent this response, all images of the catalyst surface were taken at short beam exposure times where there was no evidence of metal particle occlusion. Representative TEM images (I and II) and metal particle size distributions (based on TEM measurements, V) of reduced/passivated Au/TiO_2 (A) and Ag/TiO_2 (B) are given in Fig. 3. The TEM images of both catalysts show well-dispersed nano-scale pseudo-spheroidal metal particles. The diffractogram patterns for individual Au (AIII) and Ag (BIII) particles and the TiO_2 support (AIV and BIV) are included as insets in Fig. 3. The diffractograms for the support are consistent with anatase. The spacings (0.23 nm) between the planes in the atomic lattice for both metal particles are characteristic of the (1 1 1) plane of metallic Au (JCPDS-ICDD 04-0784) and Ag (JCPDS-ICDD 04-0783). The metal particles associated with Ag/TiO_2 present a bimodal size distribution while Au/TiO_2 is characterized by a narrower size range. However, both systems present a similar surface area weighted mean particle size (6–7 nm, see Table 1). There is an appreciable component (65% Au/TiO_2 and 45% Ag/TiO_2) of metal particles with diameters <5 nm, the particle size proposed to be crucial for catalytic activity in hydrogen-mediated reactions over Au [22,35] and Ag [39]. Taken as a whole, the characterization results demonstrate precursor reduction to the metallic form post-TPR where the Ag and Au particles exhibit a relatively narrow size distribution and similar mean size.

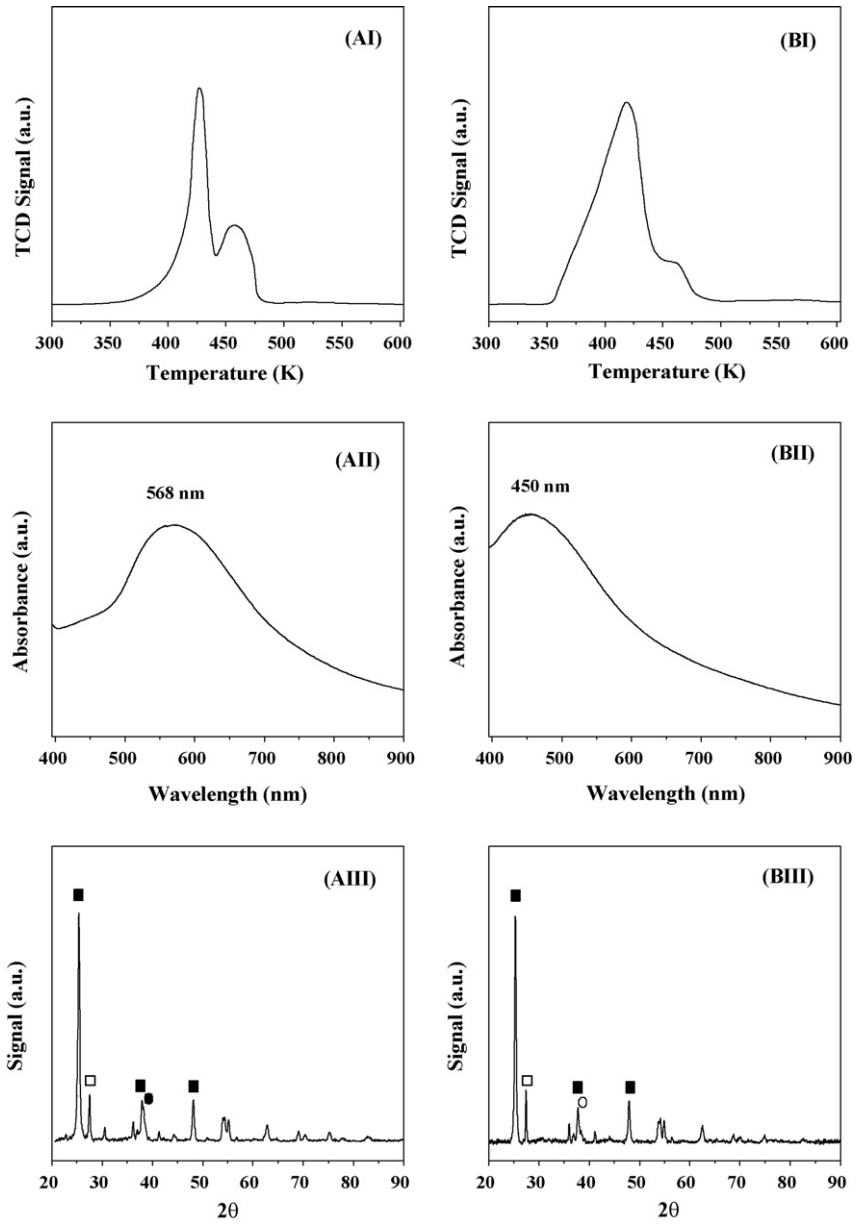

Fig. 1. Au/TiO_2 (A) and Ag/TiO_2 (B) TPR profiles (I), DRS UV–vis spectra (II) and XRD patterns (III). *Note*: XRD peak assignments based on JCPDS-ICDD reference data: (■) anatase (21-1272); (□) rutile (21-1276); (●) Au (04-0784) and (○) Ag (04-0783).

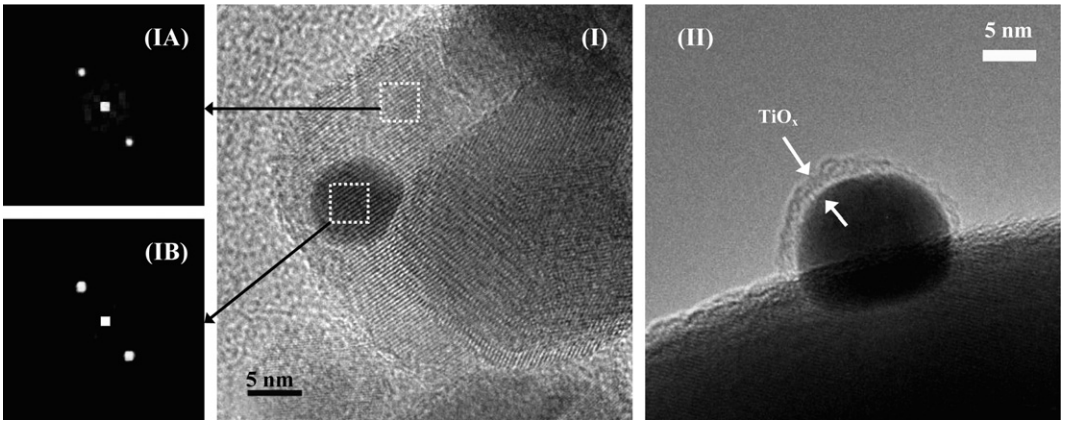

Fig. 2. Representative high-resolution TEM images of passivated/reduced (I and II) Au/TiO_2 with diffractrogam patterns (IA and IB) for the selected (dashed) areas. *Note*: Arrows in image (II) indicate TiO_x layer covering an isolated Au particle.

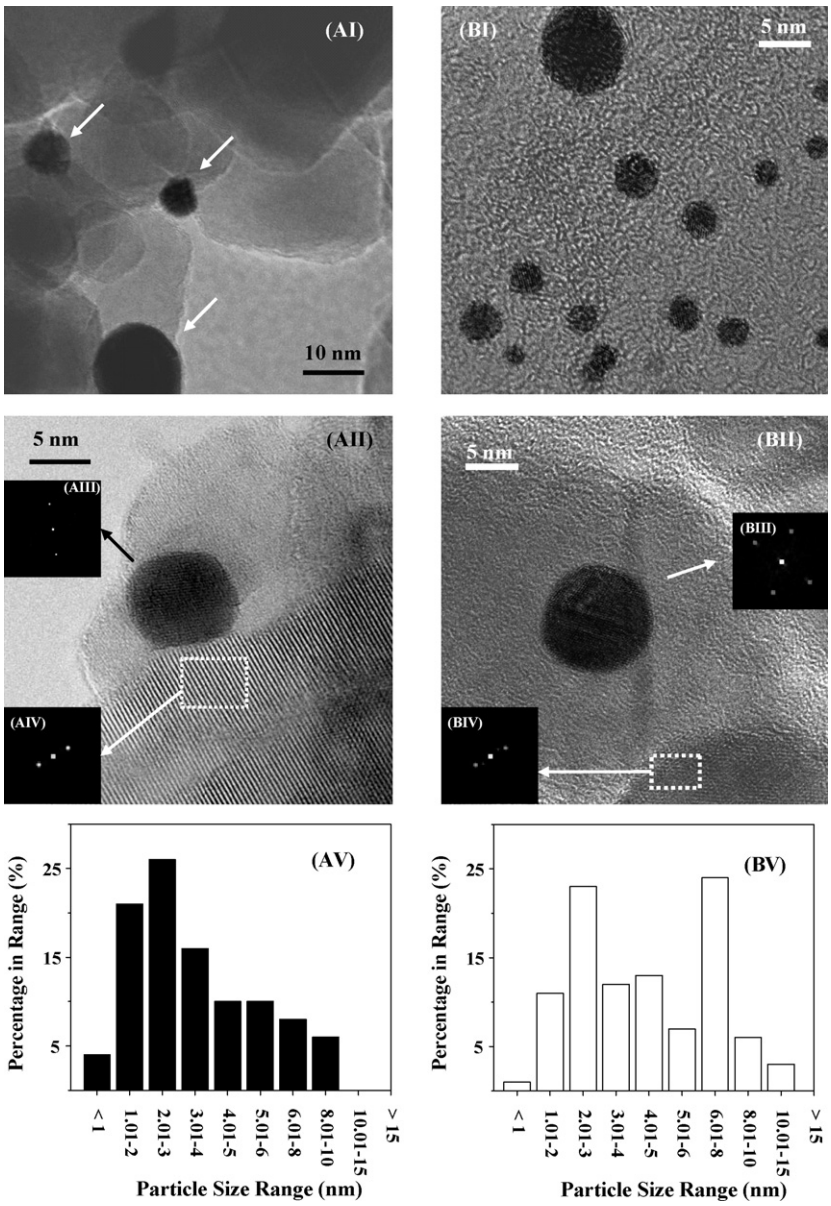

Fig. 3. Representative TEM images (I and II) and metal particle size distributions (V) of passivated/reduced Au/TiO_2 (A) and Ag/TiO_2 (B). *Note*: The diffractogram patterns of isolated metal particles (III) and TiO_2 support (IV) are included as insets.

3.2. Hydrogenation of nitrobenzene

In order to compare the catalytic response of Au *vs.* Ag in gas phase hydrogenation, we selected nitrobenzene as a reference reactant. Both catalysts promoted the exclusive formation of aniline with no evidence of hydrodenitrogenation and/or aromatic ring reduction, *i.e.* exclusive $-NO_2$ group hydrogenation. This result alone is significant in that aniline is an important chemical used as an additive for rubber production and in the manufacture of several dyes, pigments, pesticides and herbicides [1,59]. About 85% of global aniline production draws on catalytic nitrobenzene hydrogenation [60] over supported Pt [60,61] or Pd [62,63] catalysts in batch liquid operation where the formation of toxic by-products, *e.g.* nitrosobenzene [64], azobenzene [61], azoxybenzene [60,61,65] and/or phenylhydroxylamine [66], is still a major drawback associated with commercial processes. Furthermore, a time-invariant conversion was observed for both Au/TiO_2 and Ag/TiO_2, as shown in Fig. 4(I). A temporal loss of activity in the gas phase hydrogenation of nitroarenes over supported Pd [5,59,67–69] and Cu [70,71] has been reported and ascribed to the deleterious effect of H_2O as by-product [59,69], metal leaching [68] and coking [5,67,69–71]. Catalyst deactivation is also a documented feature of hydrogenation reactions over supported Au [34,72–76] and/or Ag [19,24,52] and has been linked to metal sintering [24,34,52,74], leaching [24] and carbon deposition [19,34,72,75,76].

Catalyst performance was quantified using pseudo-first order kinetics based on the mass balance under continuous flow conditions where

$$\ln\left[\frac{1}{1-x_{-NO_2}}\right] = k \times \left(\frac{n}{F_{-NO_2}}\right) \quad (3)$$

F_{-NO_2} is the total $-NO_2$ inlet molar flow, n the moles of metal in the catalyst bed: (n/F_{-NO_2}) has the physical meaning of contact time. The extracted pseudo-first order rate constants (k, units: $mol_{-NO_2}\, mol_{metal}^{-1}\, h^{-1}$) are given in Table 1. We have previously demonstrated the applicability of this approach for the hydrogenation of nitroarenes over supported Au catalysts [4,27–30] but establish here that it also applies to data generated for supported

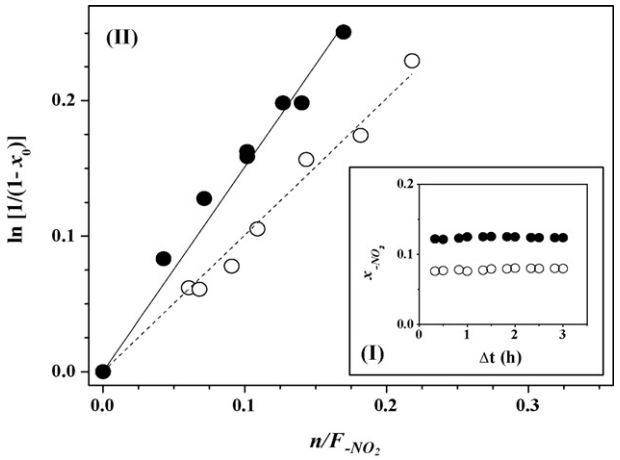

Fig. 4. (I) Variation of nitrobenzene fractional conversion (x_{-NO_2}) to aniline with time-on-stream over Au/TiO_2 (●) and Ag/TiO_2 (○) (metal/nitrobenzene = 7×10^{-2} mol_{metal} h $mol^{-1}_{-NO_2}$). (II) Pseudo-first order kinetic plot for reaction over Au/TiO_2 (●, solid line) and Ag/TiO_2 (○, dashed line) at $T = 473$ K.

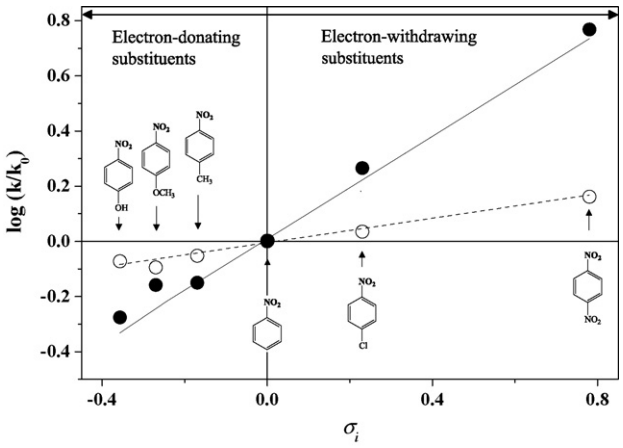

Fig. 5. Hammett plot for the selective $-NO_2$ group reduction of *para*-substituted nitroarenes over Au/TiO_2 (●, solid line) and Ag/TiO_2 (○, dashed line) at $T = 473$ K.

Ag (see Fig. 4(II)). A direct comparison of the performance of both catalysts is only meaningful in terms of specific activities, *i.e.* per m^2 of exposed metal. The Au and Ag metal surface areas were obtained from

$$S_{metal}\ (m^2_{metal}\, g^{-1}_{metal}) = \frac{6}{\rho_{metal} \times d_{TEM}} \quad (4)$$

where ρ_{metal} is the metal density and d_{TEM} is the surface area weighted mean particle size as measured by TEM. The specific pseudo-first order rate constants are included in Table 1 where it can be seen that Au delivered a measurably higher (in excess of the associated experimental error) specific hydrogenation rate when compared with Ag. We can attribute this response to a less effective activation of nitrobenzene and/or hydrogen by Ag/TiO_2 relative to Au/TiO_2. Indeed, Boccuzzi et al. [46] studied the water gas shift reaction over Ag/TiO_2 and Au/TiO_2 and ascribed the lack of activity in the case of the former to a limited capacity to activate CO.

3.3. Effect of para-substituents

The hydrogenation of nitroarenes has been proposed to proceed *via* a nucleophilic mechanism [4,7], where a weak nucleophilic agent (hydrogen) attacks the activated $-NO_2$ group with the formation of a negatively charged intermediate. In the previous section, we have noted that aniline was the only product in the hydrotreatment of nitrobenzene over both Au and Ag. In the hydrogenation of substituted nitrobenzenes bearing –OH, $-OCH_3$, $-CH_3$, –Cl and $-NO_2$ in the *para*-position, both catalysts were again 100% selective in generating the corresponding amine product. The higher activity observed for Au/TiO_2 (relative to Ag/TiO_2) in the case of nitrobenzene also extended to all the substituted nitrobenzenes where, for both catalysts, the following activity sequence was established: *p*-dinitrobenzene > *p*-chloronitrobenzene > nitrobenzene > *p*-nitrotoluene > *p*-nitroanisole > *p*-nitrophenol. In order to assess the dependence of rate on the nature of the *para*-substituent, we have applied the Hammett correlation. The Hammett equation evaluates the effect of a (*meta*- or *para*-) substituent on reaction kinetics and can be used to predict rate and equilibrium constants without prior experimental determination [77,78]. Furthermore, it is a useful tool for the elucidation of reaction mechanisms [79]. In this approach, the rate constants for the substituted reactants (k_i) can be related to that obtained for the non-substituted (or reference) benzene derivate (k_0) according to

$$\log\left[\frac{k_i}{k_0}\right] = \rho \times \sigma_i \quad (5)$$

The ρ term (reaction constant) is an estimation of the charge development during the course of the reaction and provides a measure of the susceptibility of the system to substituent electronic effects [80,81]. In a nucleophilic attack, the reaction rate is enhanced by electron-withdrawing substituents and $\rho > 0$, while ρ values close to 0 are indicative of a partially charged transition state [81]. The σ_i factor is an empirical parameter (values used in this study were taken from [79,81]) that is dependent on the substituent electron donating/acceptor character [81]. This equation was initially conceived for homogeneous systems where good linear correlations have been established for the hydrogen treatment of substituted acetophenones [82], acetamidoacrylic acid derivatives [78] and aromatic nitro-compounds [83]. The involvement of adsorption phenomena [84], the inhomogeneous distribution/nature of active sites and the greater contribution of steric effects has limited the applicability of the Hammett expression in heterogeneous catalytic systems [85]. Nevertheless, there have been some studies where it has been successfully employed in the gas [86] and liquid [87–92] phase hydrogen-mediated treatment of chlorobenzenes [86], acetophenones [87] and (of direct relevance to this study) nitroaromatics [88–92] over solid catalysts. We provide, in this report, the first example of its application to the gas phase hydrogenation of substituted nitroarenes. The fit of the experimental rate data to the Hammett relationship is presented in Fig. 5. Both catalysts generated positive reaction constants (ρ), consistent with a nucleophilic reaction mechanism. The higher ρ value generated for Au/TiO_2 (0.93) compared with Ag/TiO_2 (0.22) indicates a greater dependence of rate on the electronic character of the substituent and is diagnostic of a higher charge development in the reactant → intermediate step [81]. This, in turn, can account for the measurably higher specific activities observed for Au/TiO_2. Our ρ values are comparable to those reported for liquid phase operation (MgFeO, 0.690 [90], iron oxides 0.546 [91] and Pt/SiO_2–$AlPO_4$ 0.1–2.0 [92]), suggesting a common reaction mechanism for the formation of amines promoted by heterogeneous catalyst systems.

4. Conclusions

1 mol% Au and Ag on TiO_2 catalysts were synthesized by impregnation (with $HAuCl_4$ and $AgNO_3$) to deliver (post-TPR) a well-dispersed metallic phase, characterized by metal particles in the overall range 1–15 nm and surface area weighted mean values

of 6–7 nm. Hydrogen consumption during TPR is consistent with Au^{3+} precursor reduction to Au^0 while $AgNO_3$ undergoes a stepwise reduction to Ag^0 *via* Ag_2O. Both catalysts promoted exclusive and time-invariant $-NO_2$ reduction for a range of *para*-substituted (–H, –OH, $-O-CH_3$, $-CH_3$, –Cl and $-NO_2$) nitrobenzenes. The reaction proceeds *via* a nucleophilic mechanism where the presence of electron-withdrawing ring substituents served to elevate rate as demonstrated by the linear Hammett relationship. The higher reaction constant (ρ) obtained for Au/TiO_2 (0.93) when compared with Ag/TiO_2 (0.22) indicates a greater dependency of rate on the electronic character of the substituent and we associate this with a more effective reactant activation to generate a negatively charged intermediate leading to a higher specific rate. We provide, in this report, the first direct comparison of the catalytic action of (TiO_2) supported Au and Ag in gas phase nitroarene hydrogenation and establish the viability of both catalytic systems to promote the sustainable (continuous and clean) production of a range of commercially important amino-compounds.

Acknowledgments

The authors are grateful to Dr. W. Zhou and Mr. R. Blackley for their contribution to the TEM analysis. We acknowledge L.-A.J. Wong Fo Sue and E. Díaz for their involvement in this project. This work was financially supported by EPSRC through Grant 0231 110525. EPSRC support for free access to the TEM/SEM facility at the University of St Andrews is also acknowledged.

References

[1] P.F. Vogt, J.J. Gerulis, Ullmann's Encyclopedia of Industrial Chemistry, Wiley-VCH Verlag GmbH & Co. KGaA, Weinheim, 2005.
[2] S.G. Harsy, Tetrahedron 46 (1990) 7403.
[3] Y. Zheng, K. Ma, H. Wang, X. Sun, J. Jiang, C. Wang, R. Li, J. Ma, Catal. Lett. 124 (2008) 268.
[4] F. Cárdenas-Lizana, S. Gómez-Quero, M.A. Keane, Catal. Commun. 9 (2008) 475.
[5] V. Vishwanathan, V. Jayasri, P.M. Basha, N. Mahata, L.M. Sikhwivhilu, N.J. Coville, Catal. Commun. 9 (2008) 453.
[6] X.D. Wang, M.H. Liang, J.L. Zhang, Y. Wang, Curr. Org. Chem. 11 (2007) 299.
[7] B. Coq, F. Figuéras, Coord. Chem. Rev. 178–180 (1998) 1753.
[8] K.R. Westerterp, E.J. Molga, K.B. van Gelder, Chem. Eng. Process. 36 (1997) 17.
[9] N. Yao, J. Chen, J. Zhang, J. Zhang, Catal. Commun. 9 (2008) 1510.
[10] G. Zhang, L. Wang, K. Shen, D. Zhao, H.S. Freeman, Chem. Eng. J. 141 (2008) 368.
[11] A. Corma, P. Serna, Science 313 (2006) 332.
[12] N.S. Chaubal, M.R. Sawant, J. Mol. Catal. A: Chem. 261 (2007) 232.
[13] H. Li, Q. Zhao, H. Li, J. Mol. Catal. A: Chem. 285 (2008) 29.
[14] A. Corma, P. Serna, P. Concepción, J.J. Calvino, J. Am. Chem. Soc. 130 (2008) 8748.
[15] X.X. Han, Q. Chen, R.X. Zhou, J. Mol. Catal. A: Chem. 277 (2007) 210.
[16] X. Yang, H. Liu, H. Zhong, J. Mol. Catal. A: Chem. 147 (1999) 55.
[17] J. Słoczyński, R. Grabowski, A. Kozłowska, P. Olszewski, J. Stoch, J. Skrzypek, M. Lachowska, Appl. Catal. A: Gen. 278 (2004) 11.
[18] L. Ilieva, G. Pantaleo, I. Ivanov, A.M. Venezia, D. Andreeva, Appl. Catal. A: Gen. 65 (2006) 101.
[19] K. Theinnoi, S. Sitshebo, V. Houel, R.R. Rajaram, A. Tsolakis, Energy Fuels 22 (2008) 4109.
[20] J.E. Bailie, G.J. Hutchings, Catal. Commun. 2 (2001) 291.
[21] P. Claus, Top. Catal. 5 (1998) 51.
[22] R. Zanella, C. Louis, S. Giorgio, R. Touroude, J. Catal. 223 (2004) 328.
[23] L. Liu, B. Qiao, Y. Ma, J. Zhang, Y. Deng, Dalton Trans. (19) (2008) 2542.
[24] Y. Chen, C. Wang, H. Liu, J. Qiu, X. Bao, J.C.S. Chem. Commun. (42) (2005) 5298.
[25] J. Ning, J. Xu, J. Liu, H. Miao, H. Ma, C. Chen, X. Li, L. Zhou, W. Yu, Catal. Commun. 8 (2007) 1763.
[26] S. Jana, S.K. Ghosh, S. Nath, S. Pande, S. Praharaj, S. Panigrahi, S. Basu, T. Endo, T. Pal, Appl. Catal. A: Gen. 313 (2006) 41.
[27] F. Cárdenas-Lizana, S. Gómez-Quero, M.A. Keane, ChemSusChem 1 (2008) 215.
[28] F. Cárdenas-Lizana, S. Gómez-Quero, N. Perret, M.A. Keane, Gold Bull. 42 (2009) 124.
[29] F. Cárdenas-Lizana, S. Gómez-Quero, A. Hugon, L. Delannoy, C. Louis, M.A. Keane, J. Catal. 262 (2009) 235.
[30] F. Cárdenas-Lizana, S. Gómez-Quero, M.A. Keane, Catal. Lett. 127 (2009) 25.
[31] T. Osaki, T. Hamada, Y. Tai, React. Kinet. Catal. Lett. 78 (2003) 217.
[32] B.C. Campo, S. Ivanova, C. Gigola, C. Petit, M.A. Volpe, Catal. Today 133–135 (2008) 661.
[33] G.C. Bond, A.F. Rawle, J. Mol. Catal. A: Chem. 109 (1996) 261.
[34] T.V. Choudhary, C. Sivadinarayana, A.K. Datye, D. Kumar, D.W. Goodman, Catal. Lett. 86 (2003) 1.
[35] P. Claus, Appl. Catal. A: Gen. 291 (2005) 222.
[36] E. Bus, R. Prins, J.A. van Bokhoven, Catal. Commun. 8 (2007) 1397.
[37] B. Hammer, J.K. Nørskov, Nature 376 (1995) 238.
[38] E. Bus, J.T. Miller, J.A. van Bokhoven, J. Phys. Chem. B 109 (2005) 14581.
[39] J.-P. Deng, W.-C. Shih, C.-Y. Mou, J. Phys. Chem. C 111 (2007) 9723.
[40] J. Wambach, A. Baiker, A. Wokaun, Phys. Chem. Chem. Phys. 1 (1999) 5071.
[41] G. Tavoularis, M.A. Keane, J. Chem. Technol. Biotechnol. 74 (1999) 60.
[42] G. Yuan, M.A. Keane, Chem. Eng. Sci. 58 (2003) 257.
[43] E. Bus, R. Prins, J.A. van Bokhoven, Phys. Chem. Chem. Phys. 9 (2007) 3312.
[44] C. Baatz, U. Prüße, J. Catal. 249 (2007) 34.
[45] C. Baatz, N. Decker, U. Prüße, J. Catal. 258 (2008) 165.
[46] F. Boccuzzi, A. Chiorino, M. Manzoli, D. Andreeva, T. Tabakova, L. Ilievab, V. Iadakiev, Catal. Today 75 (2002) 169.
[47] T. Paryjczak, J. Góralski, K.W. Jóźwiak, React. Kinet. Catal. Lett. 16 (1981) 147.
[48] V.S. Kumar, B.M. Nagaraja, V. Shashikala, A.H. Padmasri, S.S. Madhavendra, B.D. Raju, K.S. Rama Rao, J. Mol. Catal. A: Chem. 223 (2004) 313.
[49] S.P. Ramnani, S. Sabharwal, J.V. Kumar, K.H.P. Reddy, K.S.R. Rao, P.S.S. Prasad, Catal. Commun. 9 (2008) 756.
[50] N. Bogdanchikova, F.C. Meunier, M. Avalos-Borja, J.P. Breen, A. Prstryakov, Appl. Catal. B: Environ. 36 (2002) 287.
[51] A. Montoya, A. Schlunke, B.S. Haynes, J. Phys. Chem. B 110 (2006) 17145.
[52] M. Bron, D. Teschner, A. Knop-Gericke, F.C. Jentoft, J. Kröhnert, J. Hohmeyer, C. Volckmar, B. Steinhauer, R. Schlögl, P. Claus, Phys. Chem. Chem. Phys. 9 (2007) 3559.
[53] G. Lee, E.W. Plummer, Phys. Rev. B 62 (2000) 1651.
[54] L. Armelao, D. Barreca, G. Bottaro, A. Gasparotto, S. Gross, C. Maragno, E. Tondello, Coord. Chem. Rev. 250 (2006) 1294.
[55] X. Jia, X. Ma, D. Wei, J. Dong, W. Qian, Colloids Surf. A 330 (2008) 234.
[56] R.I. Bickley, T. Gonzalez-Carreno, J.S. Lees, L. Palmisano, R.J.D. Tilley, J. Solid State Chem. 92 (1991) 178.
[57] S. Bernal, J.J. Calvino, M.A. Cauqui, G.A. Cifredo, A. Jobacho, J.M. Rodríguez-Izquierdo, Appl. Catal. A: Gen. 99 (1993) 1.
[58] T. Akita, M. Okumura, K. Tanaka, M. Kohyama, M. Haruta, Catal. Today 117 (2006) 62.
[59] P. Sangeetha, P. Seetharamulu, K. Shanthi, S. Narayanan, K.S. Rama Raob, J. Mol. Catal. A: Chem. 273 (2007) 244.
[60] C.-H. Li, Z.-X. Yu, K.-F. Yao, S.-F. Jib, J. Liang, J. Mol. Catal. A: Chem. 226 (2005) 101.
[61] F. Zhao, Y. Ikushima, M. Arai, J. Catal. 224 (2004) 479.
[62] E.A. Gelder, S.D. Jackson, C.M. Lok, Catal. Lett. 84 (2002) 205.
[63] X. Yu, M. Wang, H. Li, Appl. Catal. A: Gen. 202 (2000) 17.
[64] F. Zhao, R. Zhang, M. Chatterjee, Y. Ikushima, M. Araib, Adv. Synth. Catal. 346 (2004) 661.
[65] F. Ragaini, S. Cenini, M. Gasperini, J. Mol. Catal. A: Chem. 174 (2001) 51.
[66] M.M. Pérez, S. Martínez de Lecea, A.L. Solano, Appl. Catal. 151 (1997) 461.
[67] E. Klemm, B. Amon, H. Redlingshöfer, E. Dieterich, G. Emig, Chem. Eng. Sci. 56 (2001) 1347.
[68] K.K. Yeong, A. Gavriilidis, R. Zapf, V. Hessel, Catal. Today 81 (2003) 641.
[69] P. Sangeetha, K. Shanthi, K.S.R. Rao, B. Viswanathan, P. Selvam, Appl. Catal. A: Gen. 353 (2009) 160.
[70] S. Diao, W. Qian, G. Luo, F. Wei, Y. Wang, Appl. Catal. A: Gen. 286 (2005) 30.
[71] L. Petrov, K. Kumbilieva, N. Kirkov, Appl. Catal. 59 (1990) 31.
[72] B. Campo, C. Petit, M.A. Volpe, J. Catal. 254 (2008) 71.
[73] C. Milone, M.L. Tropeano, G. Gulino, G. Neri, R. Ingoglia, S. Galvagno, Chem. Commun. (8) (2002) 868.
[74] X. Zhang, H. Shi, B.-Q. Xu, Catal. Today 122 (2007) 330.
[75] B. Pawelec, A.M. Venezia, V. La Parola, S. Thomas, J.L.G. Fierro, Appl. Catal. A: Gen. 283 (2005) 165.
[76] Y. Azizi, C. Petit, V. Pitchon, J. Catal. 256 (2008) 338.
[77] L.P. Hammett, J. Am. Chem. Soc. 59 (1937) 96.
[78] M. Alamé, M. Jahjah, S. Pellet-Rostaing, M. Lemaire, V. Meille, C. de Bellefon, J. Mol. Catal. A: Chem. 271 (2007) 18.
[79] H.H. Jaffé, Chem. Rev. 53 (1953) 191.
[80] J. Shorter, Chem. Lysty 94 (2000) 210.
[81] C.D. Johnson, The Hammett Equation, Cambridge University Press, Cambridge, 1973.
[82] T. Kamitanaka, T. Matsuda, T. Harada, Tetrahedron Lett. 44 (2003) 4551.
[83] V.M. Belousov, T.A. Palchevskaya, L.V. Bogutskaya, React. Kinet. Catal. Lett. 36 (1988) 369.
[84] A. Finiels, P. Geneste, C. Moreau, J. Mol. Catal. A: Chem. 107 (1996) 385.
[85] M. Kraus, Advances in Catalysis and Related Subjects, vol. 17, Academic Press Inc., New York, 1967.
[86] T. Yoneda, T. Takido, K. Konuma, J. Mol. Catal. A: Chem. 265 (2007) 80.
[87] J.R. Ruiz, C. Jiménez-Sanchidrián, J.M. Hidalgo, Catal. Commun. 8 (2007) 1036.
[88] B. Coq, A. Tijani, F. Figuéras, J. Mol. Catal. 68 (1991) 331.
[89] P. Lu, N. Toshima, Bull. Chem. Soc. Jpn. 73 (2000) 751.
[90] P.S. Kumbhar, J. Sanchez-Valente, J.M.M. Millet, F. Figueras, J. Catal. 191 (2000) 467.
[91] M. Lauwiner, P. Rys, J. Wissmann, Appl. Catal. A: Gen. 172 (1998) 141.
[92] M.A.A. Lopidana, V.B. Bolos, C.J. Sanchidrian, J.M.M. Rubio, F.R. Luque, Bull. Chem. Soc. Jpn. 60 (1987) 3415.